Electrodynamic Magnetic Suspension—Models, Scaling Laws, and Experimental Results

Marc T. Thompson, *Member, IEEE*

Abstract—A simple experiment illustrating the principles of electrodynamic magnetic suspension is described and test results are given. A disk-shaped coil made of insulated copper magnet wire and energized with 60-Hz ac line voltage is levitated in a stable equilibrium position above a wide aluminum plate. The mechanisms generating levitation force are identified by the use of Maxwell's equations. A lumped-parameter inductance model is used to model magnetic energy storage. By using energy methods, the current necessary to achieve coil lift-off and levitation is estimated, with good results. A stability analysis is done which shows that the levitation is stable, but underdamped. Thermal models are also developed for determining temperature rise in the coil. The magnetic scaling law is developed which shows that larger magnetic structures are more efficient in energy conversion than small ones.

Index Terms—AC machines, control engineering education, eddy currents, electromagnetic fields, electromagnet heating, electromagnets, magnetic circuits, magnetic fields, magnetic levitation.

NOMENCLATURE

A	Coil surface area.
a	Coil mean radius (4.1 cm).
a_2	Coil outer radius (5.2 cm).
a_1	Coil inner radius (3 cm).
B	Magnetic flux density (Tesla).
b	Coil axial thickness (1.6 cm).
c	Coil radial thickness (2.2 cm).
c_p	Specific heat of copper, 385 J/kg-K.
C_{TH}	Thermal capacity of test coil, 135 J/K.
E_m	Magnetic stored energy (Joules).
F	Force density (N/m^2).
f_z	Axial (levitation) force (N).
F_z	Equilibrium levitation force $= Mg = 3.4$ N.
$\tilde{f}_z$	Perturbed levitation force.
g	Acceleration due to gravity (9.81 m/s^2).
h	Levitation height, from bottom of coil to top of plate.
h_c	Free convection heat transfer coefficient.
h_r	Radiation heat transfer coefficient.
I	Coil current (A).
J	Current density (A/m^2).
k_z	Magnetic spring constant (N/m).
ℓ	Coil length scale.
L_o	Inductance of coil with plate far away (980 μH).
L_r	Inductance reduction when coil location $z = 0$.
M	Mass of levitation coil (0.35 kg).
N	Coil turns ($=107$).
Q	Power dissipation in coil (W).
R_{coil}	Coil DC resistance, 0.38 Ω at 300 K.
t	Experiment time length.
ΔT	Temperature rise in coil (K).
T_A	Ambient temperature (300K).
T_{coil}	Copper coil temperature (K).
w	Conducting plate thickness (1 cm).
z	Axial position of coil above plate.
Z_o	Equilibrium position of coil above plate.
$\tilde{z}$	Perturbed coil location above plate.
μ_o	Magnetic permeability of free space $4\pi \times 10^{-7}$ H/m.
σ	Electrical conductivity $(\Omega\text{-m})^{-1}$.
δ	Skin depth (m).
γ	Decay length for inductance above plate (20 mm).
f_{osc}, ω_{osc}	Oscillation frequency of levitated coil (Hz, radians/sec).
σ_t	Stefan–Boltzmann constant, 5.668×10^{-8} W/m^{2}K^4.
α	Temperature coefficient of resistivity of copper, ≈ 0.004/K.

I. INTRODUCTION

A SIMPLE high-impact demonstration illustrating electrodynamic magnetic levitation is described. The experiment is simple, as no active control system is needed to achieve levitation of a coil in a stable equilibrium. Using this experiment, many magnetic principles such as eddy currents, induction and the Lorentz force law can be demonstrated.

Some of the more promising applications of magnetic levitation are magnetic levitation for ground transportation (low- and high-speed Maglev) [1]–[7], low friction bearings [8], magnetically levitated flywheel energy storage [9] and levitation melting [8, p. 63] of conductive metals. Other applications such as eddy-current braking [10], [11] and induction heating [12] involve similar physical processes as magnetic levitation and can be analyzed using similar techniques.

There are two types of magnetic suspensions: attractive and repulsive. In "attractive" levitation, an iron body is attracted to a source of magnetic flux. This suspension is unstable without feedback control (by Earnshaw's theorem [13]) but numerous analog and digital control techniques are available. A full-scale electromagnetic suspension (EMS) Maglev system using copper coils for generation of field is currently being tested in Germany.

In "repulsive" levitation or electrodynamic suspension (EDS), induced currents in a conducting body result in a levitation force. In EDS Maglev, a superconducting magnet that is on the moving train produces the changing magnetic flux. There
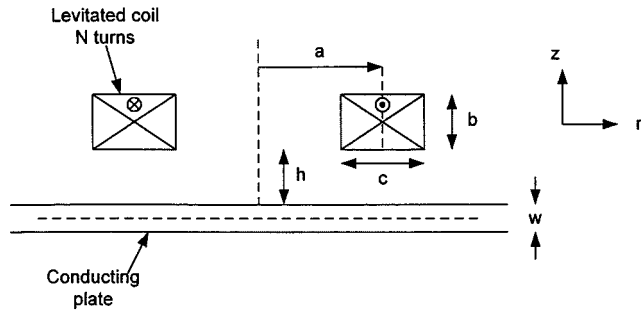
Fig. 1. Levitation experiment showing coil levitated electrodynamically above a conducting plate.

is active research in superconducting EDS Maglev with some recent efforts at the Massachusetts Institute of Technology [4]–[7], and in Japan where full-scale tests are currently being done [14].

A previous paper [15] discussed the design and demonstration of an electromagnetic levitation system, including magnet and control system design. The approach in this paper is intuitive and results are confirmed by this very simple experiment. Thermal models are also developed for determining temperature rise in the coil.

II. DESCRIPTION OF LEVITATION EXPERIMENT

The geometry of the levitation experiment is shown in Fig. 1. A circular copper coil with rectangular cross section was wound using insulated 16-gauge magnet wire and impregnated with epoxy. After curing the epoxy, the coil was placed on top of a conducting plate that is much wider than the coil. The copper coil was energized with 60 Hz AC with adjustable voltage amplitude controlled by a variable transformer. When the driving voltage was of sufficient amplitude, the coil achieved "lift-off" and levitated in a stable equilibrium at height h above the plate. By adjusting the voltage amplitude, the coil current and hence the levitation height can be adjusted.

In the following sections, the mechanisms involved in electrodynamic (EDS) levitation are identified through the use of Maxwell's equations [16]. Simplifying assumptions are identified and used to generate models for evaluating the levitation force, suspension stability and lift-off power.

A. EDS Magnetic Levitation Theory

The magnetoquasistatic (MQS) or low-frequency forms of Maxwell's equations are used to analyze this structure [17]. In MQS systems, magnetic energy storage is dominant (as compared to energy stored in the electric field) and wave phenomena are small enough to be ignored. By Ampere's law, a flowing current creates a magnetic field, or

$$\nabla \times \vec{H} \approx \vec{J} \tag{1}$$

where $\vec{H}$ is the magnetic field (Amps/meter) and $\vec{J}$ is current density (Amps/meter^2).

Faraday's law shows the mechanisms by which a changing magnetic flux generates circulating (or "eddy") currents in a conducting material. The relationship in a conducting (or

"Ohmic") material relating the current density and electric field is $\vec{J} = \sigma\vec{E}$ and can be derived

$$\frac{1}{\sigma}\nabla \times \vec{J} = \frac{-\partial\vec{B}}{\partial t}. \tag{2}$$

The term on the right of (2) is the negative of the time rate of change of the magnetic flux passing through the surface. This is the mechanism by which a changing magnetic flux impinging on a conductor creates eddy currents.

Furthermore, the Lorentz force law states that a magnetic force is created if there is a current flow in a region where there is magnetic flux, by

$$\vec{F} = \vec{J} \times \vec{B}. \tag{3}$$

Using these three principles, the mechanism for creating $+z$ lift force in this experiment is as follows.

- The ϕ-directed current in the coils generates a time-varying magnetic flux. This flux has both axial (z) and radial (r) components. Some of this flux impinges on the conducting plate below the coil.
- The changing magnetic flux impinging on the plate induces an electric field (and hence, current flow) in the conducting plate.
- The dominant current component in the plate is in the ϕ-direction. This current interacts with the r component of the magnetic field to generate lift.

B. Skin Depth, Magnetic Shielding, and Critical Frequencies

The induced currents in the plate create a reaction magnetic field that cancels the applied field. The characteristic length over which the field decays in the plate is the skin depth δ, given by

$$\delta = \sqrt{\frac{1}{\pi f \mu \sigma}} \tag{4}$$

where

f operating frequency;
μ magnetic permeability of the plate;
σ electrical conductivity of the plate.

The magnetic field inside the plate decays with this characteristic length δ, and the radial component of the field has the form

$$B_r(z) = B_r(z = 0)e^{-z/\delta} \tag{5}$$

where z is the distance from the top edge of the plate. For an ac line frequency $f = 60$ Hz and an aluminum plate with $\mu = 4\pi \times 10^{-7}$ H/m and $\sigma = 3.5 \times 10^7$ (Ω-m)$^{-1}$, the skin depth $\delta \approx 10.9$ mm. This means that an aluminum plate with thickness greater than 10.9 mm or so provides significant shielding of a 60-Hz magnetic field. A corollary to this result is that there is significant 60-Hz current in the plate, and hence a sizeable levitation force. For an operating frequency well below 60-Hz there is little induced current and very little levitation force.

III. STABILITY OF LEVIATION

Experiments show that the dynamics of the vertical suspension for electrodynamically levitated bodies are underdamped [4]–[7]. Stability of the suspension can be inferred by assuming
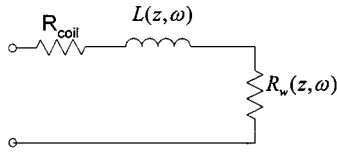
Fig. 2.   Electrical model of system

a functional dependence of the terminal inductance and using energy methods to calculate the levitation force. An electrical model for evaluating the driving point impedance of the coil is shown in Fig. 2. R_{coil} is the resistance of the coil in free-space due to the finite electrical conductivity of the wire. $L(z, \omega)$ is the frequency and geometry dependent inductance seen at the coil terminals. $R_w(z, \omega)$ is the resistance due to eddy current losses in the conducting plate. When the coil is brought near the plate, $R_w(z, \omega)$ increases and the terminal inductance of the coil decreases because the field beneath the coil is modified due to induced currents. Note that R_{coil} also has a functional dependence on operating frequency, due to the skin and proximity effects [18]. However, these effects are do not add significantly to the terminal resistance as compared to induced eddy currents in the plate.

At high frequencies, the space beneath the coil has the flux concentrated between the coil and the plate, and hence the measured coil inductance is reduced from the free-space value. Shown in Fig. 3 are the magnetic fields at dc and at 60-Hz excitation found by finite-element analysis [19]. For dc excitation the field is unperturbed by the presence of the plate (if the plate is made of nonmagnetic material). For ac excitation, there are induced currents in the conductive plate. Note the distortion of the magnetic field between the plate and the coil for 60-Hz excitation. This is due to eddy currents that are induced in the plate.

A possible functional dependence for the terminal inductance (confirmed by measurements given later in this paper) is

$$L(z) \approx L_o - L_r(\omega)e^{((-z)/\gamma)}. \qquad (6)$$

The term L_o is the terminal inductance of the coil when it is well away from the plate. The term L_r accounts for the fact that the terminal inductance decreases when the coil is near the plate, due to the induced eddy currents. The inductance is a function of the z height of the coil above the conducting plate, and decays with characteristic length scale γ. The length scale depends on the thickness of the plate and the coil dimensions, and will be determined empirically later in this paper.

In this thought experiment, assume that the coil is driven by a fixed frequency ac current source. The magnetic energy stored in the inductor is

$$E_m = \tfrac{1}{2}L(z)I^2. \qquad (7)$$

Note that even though the current is alternating, there is an average energy storage in the coil (due to the I^2 term). Since this energy varies as the coil position varies [from the $L(z)$ term], there is a resultant force acting on the coil. By the energy method the force due to an energy field can be easily calculated [20, pp. 108] and the force acting on the coil equals the negative gradient (or spatial derivative) of the energy field. In this case, the stored
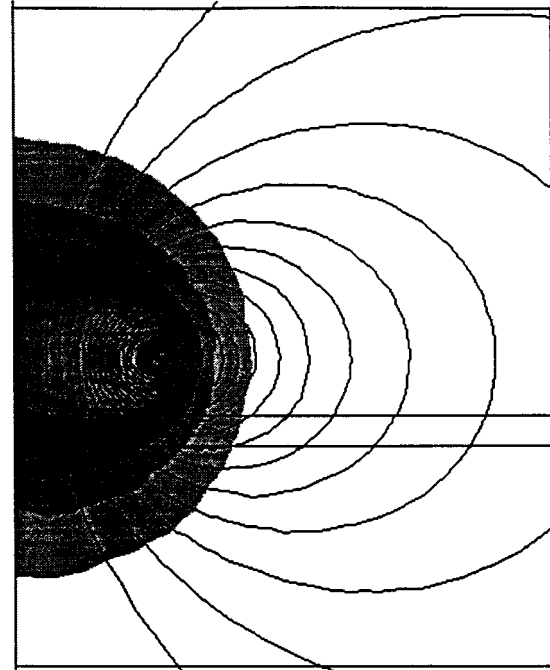
(a)
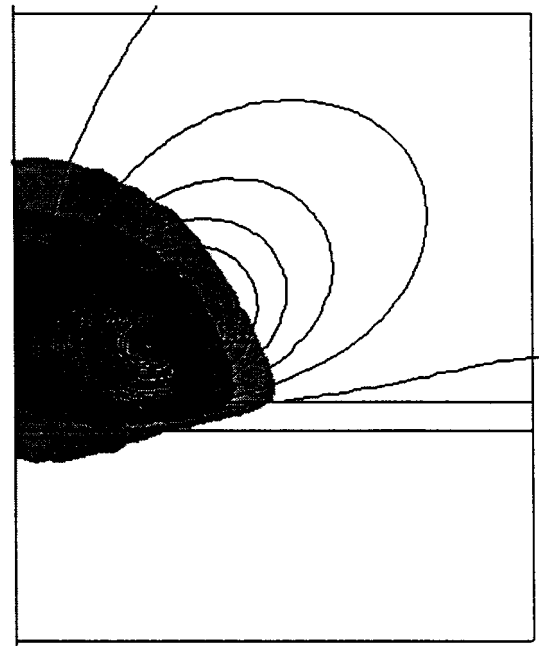
(b)

Fig. 3.   Results of finite element analysis. (a) DC. (b) 60 Hz.

magnetic energy changes as the z position of the coil varies, and the magnetic force pulls the coil toward a position of higher stored energy. The force acting on the coil in the $+z$ direction is

$$f_z = -\frac{d}{dz}E_m = \frac{I^2}{2}\frac{dL(z)}{dz} = \frac{I^2}{2\gamma}L_re^{(-z)/\gamma}. \qquad (8)$$

In order to determine the stability of the levitated coil, assume that the total levitation force acting on the coil is an equilibrium
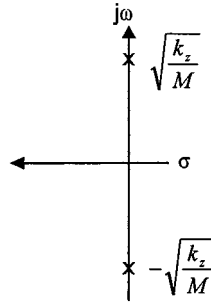
Fig. 4. Approximate pole locations for vertical mode of motion of electrodynamic magnetic suspension

TABLE I
COIL PARAMETERS

Coil mean radius	a = 4.1 cm
Coil outer radius	a_2 = 5.2 cm
Coil inner radius	a_1 = 3 cm
Coil axial thickness	b = 1.6 cm
Coil radial thickness	c = 2 cm
Coil turns	N = 107, #16 AWG copper wire
Coil inductance in free space	980 μH
Coil resistance (300K)	0.38 Ω
Coil mass	M = 0.35 kg

value plus a perturbed value, or $f_z = F_Z + \tilde{f}_z$. Also assume that the position of the coil is given by an equilibrium position, plus a small perturbation, or $z = Z_o + \tilde{z}$. By assuming that perturbations in z are small ($\tilde{z} \ll \gamma$), the force acting on the coil is

$$F_Z + \tilde{f}_z = \frac{I^2}{2\gamma} L_r e^{-(Z_o/\gamma)} e^{-(\tilde{z}/\gamma)} \approx Mg \left[1 - \frac{\tilde{z}}{\gamma}\right] \quad (9)$$

where the fact that $e^{-x} \approx 1 - x$ for $x \ll 1$ is used. Recognizing that the equilibrium force acting on the coil offsets the force of gravity (Mg) results in an expression for the perturbed force when the coil is offset from the equilibrium position

$$\tilde{f}_z = -Mg\frac{\tilde{z}}{\gamma} \equiv -k_z \tilde{z}. \quad (10)$$

A "magnetic spring constant" with value $k_z = Mg/\gamma$ is defined. Applying Newton's law to the coil results in the equation of motion for the levitated mass

$$M\frac{d^2\tilde{z}}{dt^2} + k_z \tilde{z} = 0. \quad (11)$$

For small perturbations this suspension acts like a mass acted on by a magnetic spring, and the natural frequencies of this system are on the $j\omega$ axis (Fig. 4). The frequency of oscillation for this system is given by

$$f_{osc} \approx \frac{1}{2\pi}\sqrt{\frac{k_z}{M}} \approx \frac{1}{2\pi}\sqrt{\frac{g}{\gamma}}. \quad (12)$$

This interesting result shows that it is easy to find the oscillation frequency, if one can measure (or calculate) the characteristic decay length γ of the terminal inductance.

IV. SELF-INDUCTANCE OF TEST COIL

The test coil is modeled as a round loop with rectangular cross-section, with mean radius a, axial thickness b, and trace width c. The self-inductance of this single loop is calculated using techniques outlined in Grover [21, pp. 94], where the inductance (converted to MKS units) is shown to be [22], [23]

$$L_o = \frac{25\mu_o}{\pi} aPFN^2. \quad (13)$$

This result is in MKS units, with a in meters and L_o in Henries. P and F are unitless constants; P is a function of the coil normalized radial thickness $c/2a$ and applies to a coil of zero axial thickness ($b = 0$), and F accounts for the finite axial length of the coil. For $b \ll c$ and $c \ll a$ (coils resembling thin disks) the factor $F \approx 1$, an important limiting case. Therefore, for a thin disk coil the inductance is directly proportional to radius.

For this test coil, parameters are: $a = 4.1$ cm, $b = 1.6$ cm, $c = 2.2$ cm; $c/2a = 0.268$ and $b/c = 0.727$. Using extrapolated values from *Grover*, $P = 27.92$ and $F = 0.75$, resulting in $L_o = 982$ μH. This result is very close to the measured inductance of 980 μH.

An approximate calculation for the inductance of coils with near square cross section was given in a 1928 paper by Harold Wheeler [24], where in SI units the inductance of the coil is

$$L_o = N^2 \frac{3.15a^2}{6a + 9b + 10c}. \quad (14)$$

The calculation by this method yields $L_o = 994$ μH.

The calculation of the coil inductance with the plate nearby is much more complicated; the coil inductance is both a function of vertical position and frequency. The high-frequency inductance is relatively easy to calculate if we assume that the skin depth is much smaller than the plate thickness. By the "method of images" the system at very high frequencies looks like a system with the original coil and an "image coil" on the other side of the plane. If the mutual inductance between the two coils is found, the self-inductance of the primary coil is easily calculated [25]. However, this simple calculation is not valid at intermediate frequencies (less than a few hundred Hz for this system) and an empirical approach was adopted by directly measuring the 60 Hz inductance with the coil at different heights above the plate.

V. EXPERIMENTAL RESULTS

A 1-cm thick aluminum plate was used for inductance measurements and levitation experiment. Parameters of the copper test coil are given in Table I.

A. Coil Inductance Measurements

The coil inductance at 60 Hz and for various heights above the conducting plate was measured using a Hewlett–Packard HP4192A impedance analyzer. The inductance was measured for coil heights of 0, 5, 10, 15, and 20 mm above the plate
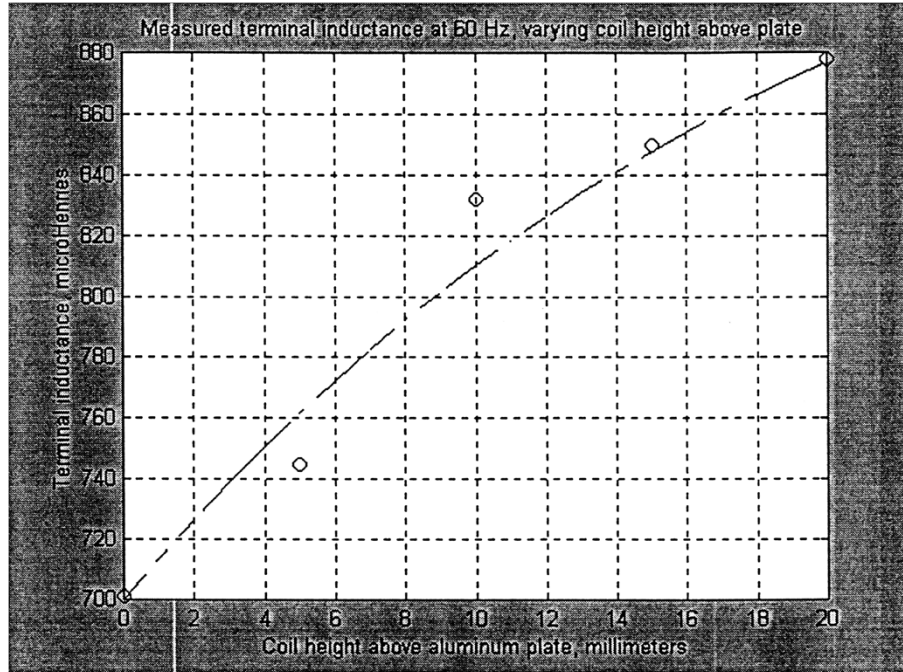
Fig. 5.   The 60 Hz coil inductance for various coil heights above aluminum plate. Dotted line is curve fit to data.

TABLE II
CURVE FIT PARAMETERS FOR TERMINAL INDUCTANCE

L_o	980 μH
L_r	280 μH
γ	20 millimeters

(Fig. 5). The data was curve fit to our terminal inductance expression (6), with the parameters for the curve fitting shown in Table II. This data was used to estimate the minimum current needed for coil lift-off, power dissipation, and the resonant frequency of the suspension.

B. Coil "Lift-Off" Power and Levitation Height

Since the terminal inductance is now known, the current needed to achieve levitation can be easily estimated. By the energy method, the necessary current to achieve lift-off is calculated to be

$$I = \sqrt{\frac{2Mg}{[dL(z)/dz]_{z=0}}} = \sqrt{\frac{2(0.35)(9.81)}{0.014}} = 22.1 A(\text{RMS})$$

(15)

For this calculation, the term $dL(z)/dz$ evaluated at $z = 0$ results in $L_r/\gamma = 0.014$ H/m. The measured current to achieve lift-off was approximately 21 A (RMS), with 26 A resulting in 10 mm levitation height (Fig. 6), and 39 A resulting in 20 mm levitation height. The lift-off power needed is approximately 168 W, with 257 W needed to levitate at $h = 10$ millimeters and 578 W needed at $h = 20$ mm. A summary of measured and calculated current needed at a given levitation height is given in Table III.
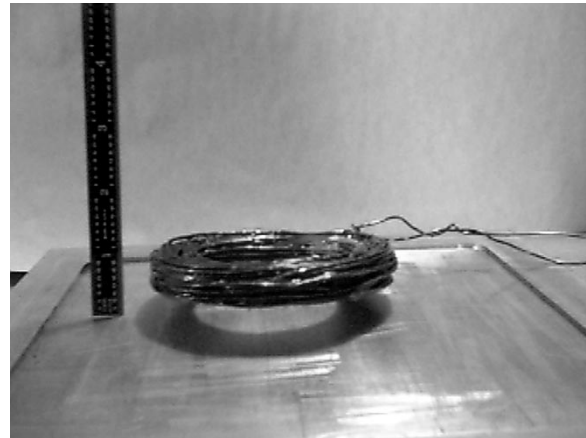
Fig. 6.   Coil levitated approximately 10 mm above aluminum plate

TABLE III
PREDICTED AND ACTUAL COIL CURRENT VS. LEVIATION HEIGHT, AND
CALCULATED POWER DISSIPATION IN COIL

h (mm)	$I_{measured\ (A\text{-}RMS)}$	$I_{calc\ (A\text{-}RMS)}$	Q (Watts)
0	21	22.1	168
10	26	28.4	257
20	39	36.5	578

C. Resonant Frequency of Suspension

The curve fit shows that the characteristic decay length for inductance is approximately 20 millimeters. Therefore, our estimate for resonant frequency is

$$f_{osc} \approx \frac{1}{2\pi}\sqrt{\frac{g}{\gamma}} \approx \frac{1}{2\pi}\sqrt{\frac{9.81}{0.02}} \approx 3.5\ \text{Hz.}$$

(16)

The coil was levitated at a height 10 mm above the plate and was allowed to bounce vertically. A resonant frequency of approximately 4 Hz was measured.

D. Thermal Models and Coil Temperature Rise

A simple thermal model is used to calculate the temperature rise of the coil under various test conditions. If the coil is levitated for a long time a static model is appropriate; the heat loss (Q, W) by convection and radiation from the coil surface is

$$Q = (h_c + h_r)A(T_{coil} - T_A). \qquad (17)$$

The free convection heat transfer coefficient (h_c) is approximately 0.001 W/cm^2-K [26] and the surface area of the test coil $A = 196$ cm^2. The radiation heat transfer coefficient is more difficult to calculate, as radiation loss depends on the forth power of the absolute coil temperature. The radiation heat transfer coefficient may be expressed as [26]

$$h_r = \frac{\sigma_t \varepsilon (T_{coil}^4 - T_A^4)}{(T_{coil} - T_A)} \qquad (18)$$

where σ_t is the Stefan–Boltzmann constant and $\varepsilon \approx 0.10$ is the emissivity of the copper material. With ambient temperature $T_A = 300$K, the radiation heat transfer coefficient increases from 0 to 0.0008 W/cm^2-K over the temperature range 300–1000K; clearly free convection will dominate here. The temperature rise calculated (if we wait a long time) at a levitation height of 10 mm with $Q = 168$ W is >500K. Clearly, the experiment cannot be run for very long or the coil will be damaged by thermal stresses.

A better approach is to run the coil for a short period of time and to allow it to cool between experiments. In this case, the temperature rise of the coil can be approximated if the thermal capacity of the coil (C_{TH}, in Joules/K), the power dissipation, and the experiment time are known. For copper, the specific heat $c_p = 385$ Joules/kg-K and hence the thermal capacitance of the coil is $C_{TH} = Mc_p = 135$ Joules/K. The approximate temperature rise in the coil in a 30-s experiment at $h = 10$ mm is

$$\Delta T \approx \frac{Qt}{C_{TH}} = \frac{(168 \text{ J/s})(30 \text{ s})}{135 \text{ J/K}} \approx 37\text{K}. \qquad (19)$$

This is a reasonable result, as this temperature rise is unlikely to cause injury or coil damage. Obviously the experiment should be run for less time at a higher levitation height, due to the higher power dissipation required.

Note that at high temperature the current needed to levitate is even higher, as the coil resistance increases with temperature, as

$$R_{coil}(T) = R_{coil}(T = 300\text{K})[1 + \alpha(T - 300)] \qquad (20)$$

where $\alpha \approx 0.004$ is the temperature coefficient of the resistivity of copper. For example, a 100K temperature rise in the coil results in $\sim$40% increase in coil resistance.

E. Magnetic Scaling Laws

Magnetic scaling laws [4] show that large magnetic elements are more efficient in energy conversion than smaller ones. Conversely, small-scale levitation experiments are likely to be very power hungry (or unable to levitate at all before they burn up, as shown in the previous section). For the test coil, this effect can be quantified by considering the ratio of the lift force to the power dissipation. For the thin disk coil, the inductance L is approximately proportional to a, the coil radius [21]–[23]. The lift force is proportional to $dL(z)/dz$, which is also proportional to the coil radius a. The power dissipation is proportional to the resistance of the coil, which in turn is proportional to a/bc, the ratio of current path length to coil cross-sectional area. Therefore, the ratio of lift force to power loss is proportional to bc, or the cross-sectional area of the coil. If all coil lengths are scaled up by the same factor ℓ, the ratio of lift force to power dissipation increases by the factor ℓ^2, or the length squared.

To achieve lift-off of the test coil in this experiment, approximately 168 W is dissipated in the coil. Furthermore, as the coil heats up, more power must be dissipated for the same levitation height, since the winding resistance increases with temperature. So, the test coil gets hot, and can only be run for a few seconds at a time. As shown by the magnetic scaling laws a larger coil could be levitated for longer periods of time.

VI. CONCLUSIONS

This paper presents a simple demonstration of electrodynamic magnetic levitation using a small copper coil, energized with 60-Hz ac and levitated stably without feedback over an aluminum plate. The processes that generate magnetic forces are identified using Maxwell's equations. Through a thought experiment, a method for determining lift-off power, levitation height, and suspension resonant frequency is shown. After measuring the terminal inductance using an impedance analyzer, the lift-off current and suspension resonant frequency was estimated by applying energy methods to the suspension. The simple models derived give good agreement with the measured lift-off power and suspension resonant frequency. A thermal model shows how long the experiment can be run without the coil exceeding a specified temperature rise. The principles outlined in this paper have application to magnetic levitation, induction heating and other electrodynamic processes involving induced eddy currents.

REFERENCES

[1] J. R. Powell and G. R. Danby, "High speed transport by magnetically suspended trains," *ASME Pub. 66 WA/RR5*, Dec. 1966.
[2] C. A. Guderjahn, S. L. Wipf, H. J. Fink, R. W. Boom, K. E. MacKenzie, D. Williams, and T. Downey, "Magnetic suspension and guidance for high speed rockets by superconducting magnets," *J. Appl. Phys.*, vol. 40, no. 5, pp. 2133–2140, April 1969.
[3] H. H. Kolm and R. D. Thornton, "The magneplane: Guided electromagnetic flight," in *Proc. 1972 Appl. Superconductivity Conf.*, May 1–3, 1972.
[4] M. T. Thompson, "High temperature superconducting magnetic suspension for maglev," Ph.D. dissertation, Dept. Elect. Eng. Comput. Sci., Mass. Inst. Technol., Cambridge, May 1997.

[5] M. T. Thompson and R. D. Thornton, "Modeling of HTSC based iron-core flux-canceling electrodynamic suspension for maglev," in *Proc. 4th Int. Symp. Magn. Suspension Technol.*. Gifu, Japan: NASA Conf. Pub., 1997.

[6] M. T. Thompson, R. D. Thornton, and A. Kondoleon, "Scale model flux-canceling EDS Maglev suspension—Part I: Design and modeling," *IEEE Trans. Magn.*, vol. 35, no. 3, May 1999.

[7] M. T. Thompson and R. D. Thornton, "Scale model flux-canceling EDS Maglev suspension—Part II: Test results and scaling laws," *IEEE Trans. Magn.*, vol. 35, May 1999.

[8] P. J. Geary, *Magnetic and Electric Suspensions*: Brit. Sci. Instr. Res. Assoc., 1964.

[9] T. Clark, A. Kondoleon, M. Thompson, and R. Thornton, "Shaftless, magnetically levitated flywheel energy storage system," in *Aerospace Flywheel Workshop*, Albuquerque, NM, Oct. 7–8, 1998.

[10] H. D. Wiederick, N. Gauthier, D. C. Campbell, and P. Rochon, "Magnetic braking: Simple theory and experiment," *Amer. J. Phys.*, vol. 55, pp. 500–503, 1987.

[11] M. T. Thompson, N. LaWhite, and E. M. Pribonic, "Permanent magnet eddy current brakes—Design principles, scaling laws and prototype test fixture results," Trans. Magn., 2000, submitted for publication.

[12] M. Adler, "A field-theoretical approach to magnetic induction heating of thin circular plates," *IEEE Trans. Magn.*, vol. MAG-10, pp. 1118–1125, Dec. 1974.

[13] S. Earnshaw, "On the nature of the molecular forces which regulate the constitution of the luminiferous ether," *Trans. Cambridge Philos. Soc.*, vol. 7, pp. 97–112, 1842.

[14] [Online] Available http://www.rtri.or.jp.

[15] W. G. Hurley and W. H. L. Lolfle, "Electromagnetic design of a magnetic suspension system," *IEEE Trans. Educ.*, vol. 40, pp. 124–130, May 1997.

[16] J. C. Maxwell, *Electricity and Magnetism*. New York: Dover, 1954, vol. 1–2.

[17] H. A. Haus and J. R. Melcher, *Electromagnetic Fields and Energy*. Englewood Cliffs, NJ: Prentice-Hall, 1989.

[18] R. W. Erickson, *Fundamentals of Power Electronics*. Boston, MA: Kluwer, 1999.

[19] D. Meeker. Finite element method magnetics. FEA program. [Online] Available http://members.aol.com/gmagnetics/download.htm.

[20] A. E. Fitzgerald, C. Kingsley Jr., and S. D. Umans, *Electric Machinery*, 5th ed. New York: McGraw-Hill, 1990.

[21] F. W. Grover, *Inductance Calculations: Working Formulas and Tables*. New York: Dover, 1946.

[22] M. T. Thompson, "Inductance calculation techniques—Part I: Classical methods," *Power Contr. Intell. Motion*, vol. 25, no. 12, pp. 40–45, December 1999.

[23] M. T. Thompson. Inductance calculation techniques—Part II: Approximations and handbook methods. *Power Contr. Intell. Motion* [Online] Available website http://www.pcim.com.

[24] H. A. Wheeler, "Simple inductance formulas for radio coils," in *Proc. IRE*, Oct. 1928, vol. 16.

[25] W. G. Hurley and M. C. Duffy, "Calculation of self and mutual impedances in planar magnetic structures," *IEEE Trans. Magn.*, vol. 31, pp. 2416–2422, July 1995.

[26] B. V. Karlekar and R. M. Desmond, *Engineering Heat Transfer*. St. Paul, MN: West, 1977.

Marc T. Thompson (M'92) was born in Vinalhaven Island, Maine. He received the B.S.E.E., M.S.E.E., and the Ph.D. degrees from the Massachusetts Institute of Technology, Cambridge.

He is President of Thompson Consulting and Adjunct Associate Professor of electrical engineering at Worcester Polytechnic Institute (WPI), Worcester, MA. At WPI, he teaches intuitive methods for analog circuit, magnetic, thermal and power electronics design. His main research at MIT concerned the design and test of high-temperature superconducting suspensions for MAGLEV an the implementation of magnetically based ride quality control. Other areas of his research and consulting interest include planar magnetics, power electronics, high speed analog design, induction heating, IC packaging for improved thermal and electrical performance, use of scaling laws for electrical and magnetic design, and high-speed laser diode modulation techniques. He has worked as a consultant in analog, electromechanics, mechanical and magnetics design, and holds two patents. Currently he works on a variety of consulting projects, including high-power and high-speed laser diode modulation, eddy- current brake design for amusement applications, flywheel energy storage for satellites, and magnetic tracking for interbody catheter positioning and is a consultant for Magnemotion, Inc., United States Department of Transportation, Magnetar, Inc., and Polaroid Corporation.